MLM-MU-79-70-0027



# ANALYTICAL STUDY OF TATB PREHEATING METHODS

By

Tien S. Chou

RECEIVED
JUL 01 1996
OSTI



October 29, 1979

Monsanto

**MOUND FACILITY**
Miamisburg, Ohio 45342

operated by
**MONSANTO RESEARCH CORPORATION**
a subsidiary of Monsanto Company

for the
**U. S. DEPARTMENT OF ENERGY**

Contract No. DE-AC04-76-DP00053

MLM-MU-79-70-0027

# ANALYTICAL STUDY OF TATB PREHEATING METHOD

By

Tien S. Chou

## DISCLAIMER



**MOUND FACILITY**
Miamisburg, Ohio 45342

operated by
**MONSANTO RESEARCH CORPORATION**
a subsidiary of Monsanto Company

for the
**U. S. DEPARTMENT OF ENERGY**

Contract No. EY-76-C-04-0053

TABLE OF CONTENTS

## INTRODUCTION

TATB (1,3,5 - triamino 2,4,6 - Trinitrobenzene) is a very stable explosive that is remarkably insensitive to severe impact and thermal environment. Experiments on its initiation and detonation characteristics (Ref. 1) have found it difficult to initiate under the energy transfer of thin flyer plates accelerated by electrically exploded metal foils. Figure 1 shows the propagation of a detonation front in such an experiment. Generally, the detonation waves are confined in the region directly in front of the flyer impact surface, leaving a substantial portion of the HE undetonated. It has been suggested by Lawrence Livermore personnel that a preheated TATB charge may improve its sensitivity and thus reduce or eliminate this deficiency.

The above experiments were performed at the sample temperatures ranging from -54° to +74°C. As the temperature was lowered while the flyer impact velocity remained the same, a pronounced increase in the curvature of the detonation front was observed. This results in a significant decrease in the divergence of the detonation wave. Although an accurate relationship between the wave front divergence and the sample temperature is not available, it is generally believed that, due to an accelerated rate of chemical reaction, the detonation will significantly improve at higher temperatures. It is assumed that desired results may be obtained if we preheat the TATB to 100°C at a depth of 1 cm from the flyer impact surface.

Many parameters influence the methods to be considered for carrying out this HE preheating. The most important among them are the time allowed and the amount of energy available. The task is made extremely difficult by the fact that TATB is a poor thermal conductor and that deflagration occurs at around 250°C. In this study, we investigate several heating arrangements and predict the temperature distributions under prescribed boundary conditions.

### Basic Models and Analyses

The thermal properties of TATB are assumed homogeneous and constant throughout the temperature range of 20 to 250°C. The heat capacity is C = 0.030 cal/gm°C, the thermal conductivity k = 0.0025 cal/sec cm °C, and the density is also constant at $\rho$ = 1.9 gm/cc. The HE charge holder is made of ceramic material with the following constant properties: heat capacity at 0.21 cal/gm °C, thermal conductivity at 0.05 cal/sec cm °C and density at 2.0 gm/cc.

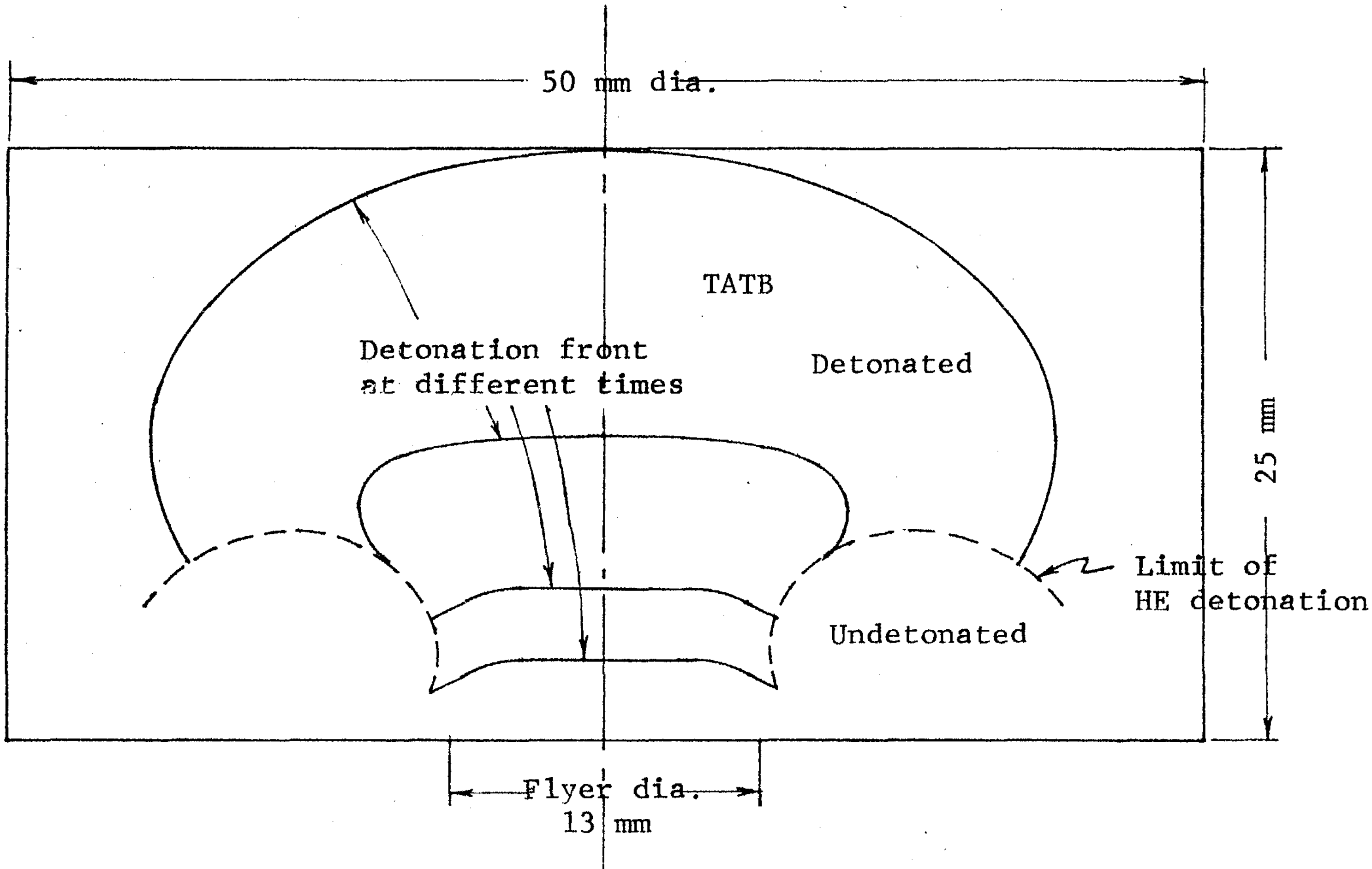


Fig. 1. Propagation of a detonation front in TATB

With the properties given, a theoretical minimum required time can be readily obtained. From Figure 1, we see that the only location feasible for a heat source is the bottom of the charge holder. If the thickness of the TATB is to reduce to 2 cm, we have in approximation, an infinite plate thermal model with a simple analytical solution. Consider an infinite plate of thickness L, having an initial uniform temperature of $t_i$. If the temperature of both surfaces is raised to $t_1$ and remains there from the time $\tau = o$ on, then the temperature distribution is given by (Ref. 2).

$$\frac{t(x,\tau) - t_1}{t_i - t_1} = \frac{4}{\pi} \sum_{n=1}^{\infty} \frac{1}{n} \exp -\left(\frac{n\pi}{2}\right)^2 \theta \quad \sin \frac{n\pi}{L} x$$

$$n = 1, 3, 5 \ldots\ldots$$

where: $\theta = \frac{4\alpha}{L^2} \tau$

$\alpha = \frac{k}{\rho c}$ the diffusivity

and x is the transverse distance form the bottom surface.
The TATB is orginally at 20$^{o}$C and is suddently brought in contact with an infinite heat source at 250$^{o}$C, the deflagration temperature. Thus, we have L = 2 cm, $t_i$ = 20$^{o}$C and $t_1$ = 250$^{o}$C. We are looking for $\tau_o$ the time required for the center of the TATB slab to reach t (L/2, $\tau_o$) = 100$^{o}$C. The dimensionless temperature is -

$$\frac{t(L/2, \tau_o) - t_1}{t_i - t_1} = 0.652$$

From Figure 10-2 and Table A-8 of Ref (2) we obtain, for x/L = 0.5, O = 0.271. With a diffusivity of $\sigma$ = 0.263 cm$^2$/min, this gives $\tau_o$ = 1.03 min. This is the shortest time required to heat TATB from 20$^{o}$C to 100$^{o}$C at 1 cm depth, if the surface temperature is not to exceed 250$^{o}$C. A similar calculation with the surface temperature maintained at 200$^{o}$C give $\tau_o$ = 1.28 min. The desired preheating time is somewhere around 20 secs. Thus an improved heating method is needed.

It should be noted that the above model represents ideal conditions and in practice it is impossible to maintain the surface at a given temperature at all times. The values thus obtained are only estimates of times.

required to heat the respective models. In order to obtain a better prediction, we proceed to analyze the system with a numerical method, using finite-difference approximation (Ref 2). A semi-infinite slab of TATB is placed on top of a ceramic plate of 0.38 cm thickness. At the center of the plate, there is a circular barrel of 0.48 cm diameter for the travel of a slapper. A heat source is optimally embedded in the plate surrounding the barrel. The TATB and the ceramic are represented by a network of hollow concentric circular grids. A set of difference equations and boundary conditions thus allow a numerical solution of the transient heat transfer problem.

The rate of heat input at the heat source is obtained by trail and error, with the peak TATB temperature kept below the deflagration temperature. The heat transfer at the contact surface of two materials is approximated by a constant coefficient of 1.2 cal/sec-cm$^2$-$^o$C. An optimum result is obtained with the following rates of heat input.

| | |
|---|---|
| 660 cal/min for | $\tau$ = 0 - 0.5 min |
| 250 cal/min | 0.5 - 3.0 min |
| 200 cal/min | 3.0 - 6.0 min |

The temperature histories at two representative locations are plotted in Figure 2.

Since the ceramic charge holder is a much better heat conductor than TATB, the temperature at the TATB surface in contact with the charge holder rises sharply immediately, and reaches 250$^o$C within half a minute. The interior temperature at 1 cm depth rises much slower due to the high heat capacity and low thermal conductivity of TATB. At the end of the half minute period, it reaches only about 27$^o$C. To avoid deflagration, we reduce the rate of heat input to 250 cal/min at this point. As expected, the interface temperature responds instantly, dropping almost 30$^o$C before rising again. This temperature drop is attributed mainly to large temperature gradients in the TATB charge. The interior temperature begins to rise significantly and, at the end of the three minute period, reaches 94$^o$C. The heating rate is further reduced to 200 cal/min, thus holding the interface temperature below 250$^o$C for the next three minutes. The interior temperature reaches the proposed firing temperature of 100$^o$C in approximately four minutes.

The required time of more than three minutes in this model is substantially longer than 1.03 minutes predicted by the analytical solution primarily because of the following factors. First of all,

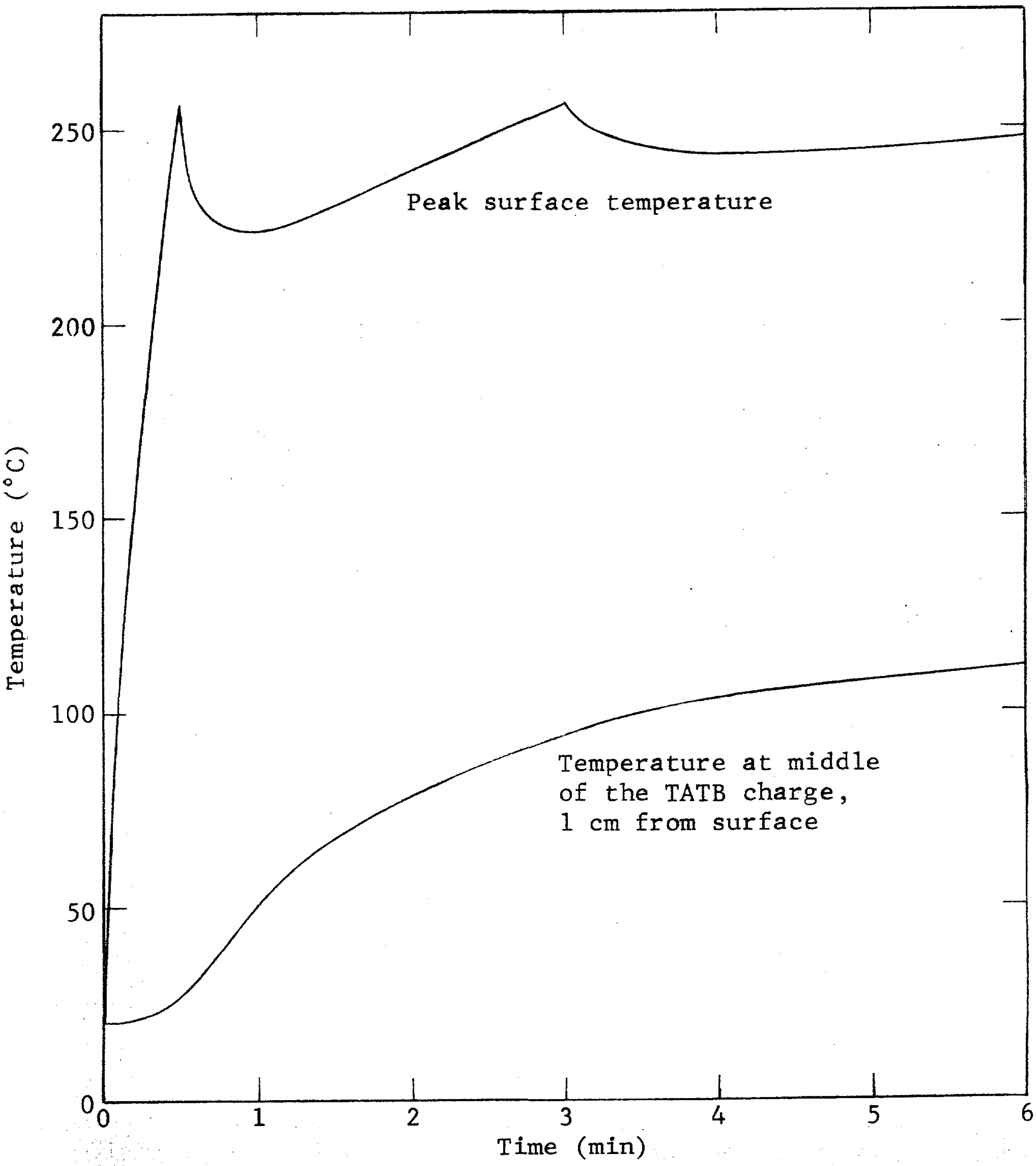


Fig. 2. TATB temperature history in the one-dimensional model

it is difficult to raise the interface temperature to 250°C fast and then maintain it at that point throughout the heating period. Furthermore, the heat loss into the large TATB heat sink makes the temperature rise much more difficult. The influences of the thermal contact resistance at the interface and thermal resistance within the ceramic charge holder are minor by comparison.

Charge Holder Configuration

Barring a premixing of the TATB charge to improve its thermal conductivity, we have limited means of accelerating the preheating. Important among them are the geometry, conducting media and insulators. Figure 3 shows a modified system incorporating these improvements. A ceramic charge holder contains a truncated conical cavity of 1.2 cm dia. on the top and 0.8 cm dia. on the bottom. The cavity is filled with TATB to be heated to 100°C prior to detonation. At the top end of the cavity, two aluminum discs facilitate heat transfer to the TATB in that region. In addition, a spherical plastic heat shield reduces excessive heat loss into the main TATB mass above the cavity.

The modified charge holder configuration alone, without the conductor discs or the heat shield, provides multiple paths for heat conduction into the region of TATB that is crucial to efficient detonation. As the numerical solutions will show, this change alone significantly improves the heating process. However the TATB in the critical region reaches only 40°C in 10 secs. The addition of the aluminum discs shows a better improvement, raising the same temperature to 100°C in around 10 secs. However, the discs being embedded in the TATB charge may have an adverse effect on the detonation process. The heat shield is rather ineffective by comparison. In addition, by maintaining the main body of the TATB charge close to the room temperature it may not have contributed to the overall detonation efficiency to a great extent.

For the following analyses, the thermal properties of aluminum and plastic are assumed constant in the temperature range under consideration. The density, the heat capacity and the thermal conductivity of the aluminum are respectively 2.7 gm/cc, 0.18 cal/gm °C and 0.48 cal/sec cm °C. The thermal conductance per unit area of plastic is assumed at 0.04 cal/sec $cm^2$ °C.

As is in the previous simple model, a set of heat sources is optimally placed within the ceramic. Because of its high thermal conductivity, the distribution of the heat sources is not critical. The peak TATB temperature exists at the interface of the ceramic and the TATB. Usually, it is at or near the bottom of the cavity. The temperature in this region limits the rate of heat input.

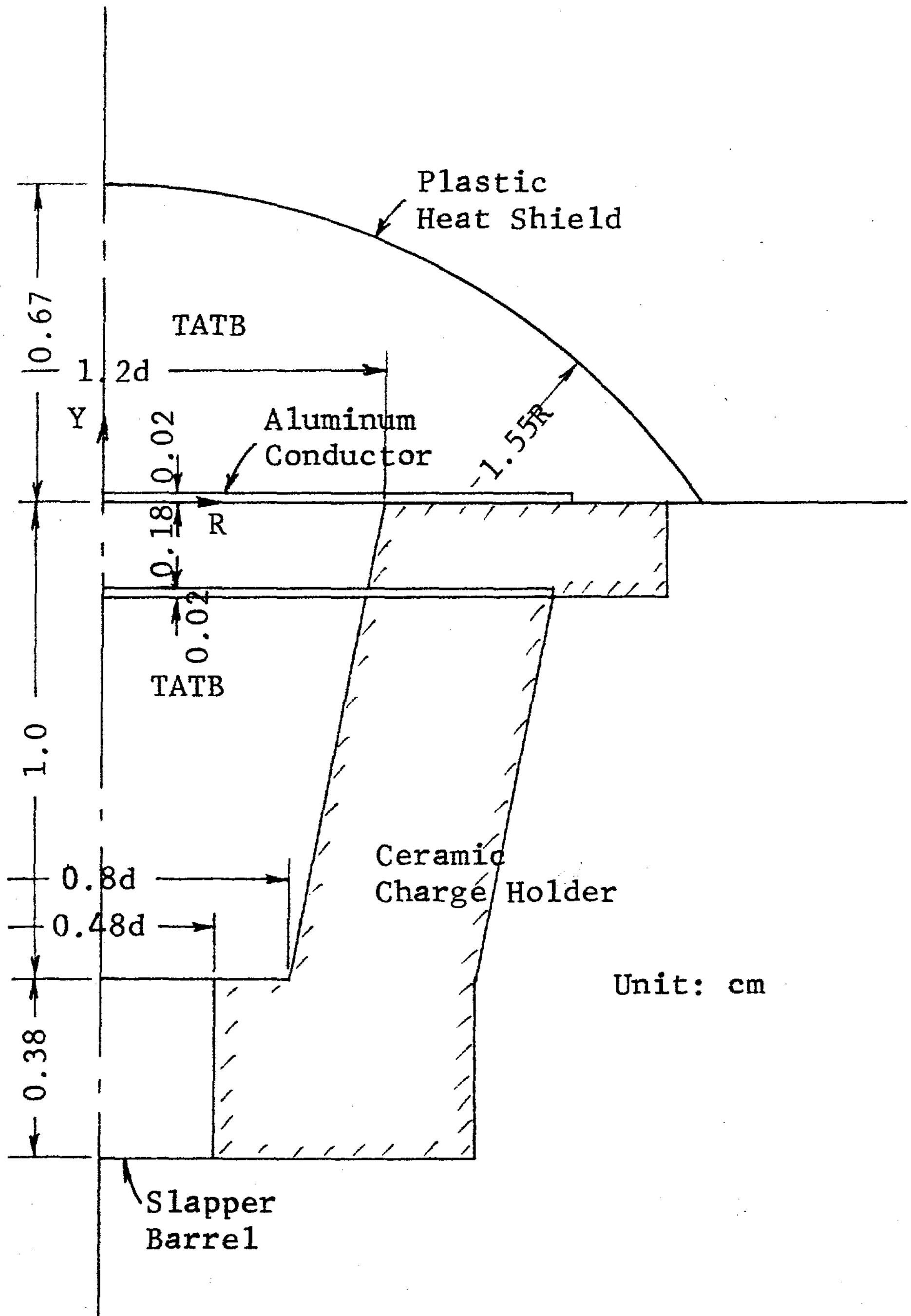


Fig. 3. Modified charge holder with alminum conductors and plastic shield

## Analytical Results and Discussions

In order to perform the numerical analyses, the system shown in Figure 3 is divided into a network of small elements. Each element is a hollow concentric circular disc of small dimensions in R and Y. The differential equations governing the heat transfer are transformed into a set of difference equations. These equations are then solved together with a given set of boundary conditions to arrive at the transient temperature distributions. For the boundary condition, the system is initially set at a room temperature of 20°C. The rate of heat input is obtained by trial and error while maintaining the TATB peak temperature at below 250°C.

The results of these heat transfer analyses are given in Figures 4-15. In order to study the effects of the various parameters mentioned, we analyzed the system in Figure 3 with four variations. The first variation deals with heat transfer process with neither the shield nor the conductors. Since the alterations in the system affect the interface temperature, the rates of heat input are consequently different. To faciliate comparisons, each heat input starts at a high rate for the first 8 secs and then drops to a lower level to maintain the interface temperature close to 250°C while allowing the interior temperature to rise. As seen in Figure 4, the peak interface temperature reaches 243°C after 8 secs of 42 cal/sec heat input. The values given for the coordinates R and Y identify the locations of material according to Figure 3. Of interest to us is the temperature at (0.1, 0.1 cm), which reaches only 25°C at this point.

As the rate of heat input drops to 12 cal/sec, the interface temperature stabilizes. The temperature at (0.1, 0.1 cm) reaches 51°C at 15 secs. The temperature distributions of the entire system at 15 secs are plotted in Figures 5 and 6. Generally, as seen in Figure 5, the temperature is lower near the center line due to the greater distances of heat conduction paths to the charge holder. It rises sharply toward the interface. For positive Y locations, which represent the TATB in the main region outside the cavity, the temperatures peak at around R = 0.8 cm and drop off sharply. This is obviously due to the heat dissipation into the surrounding heat sinks. Figure 6 gives the temperature profiles in the Y direction at given R values. The great negative gradients indicate the difficulty in dissipating into the TATB main body.

In order to examine the effect of the aluminum conductors on the heat transfer process, we include in the next analyses one and two conductors respectively. In the case of one conductor, the top one shown in

Figure 3 is removed. In the same manner, the results are shown in Figures 7 through 12. The system with one conductor calls for 43 cal/sec heat input rate in the first 8 secs and 12.5 cal/sec thereafter. Here, at 15 secs, the temperature at (0.1, 0.1 cm) reaches 88$^oC$. Clearly, the conductor forces an accelerated heat transfer in this region. The axial temperature profile given in Figure 9 peaks at the conductor which is located at Y = -0.2 cm. Generally, the TATB temperatures in the cavity are above 150$^oC$ at 15 secs.

The second conductor has the same effect as the first one. The heat input rate for the first 8 secs is increased to 45 cal/sec. As seen in Figures 10 through 12, the temperatures are generally higher. A large extent of the TATB near the cavity exceeds the desired temperature of 100$^oC$. As expected, a third set of peak temperatures is seen in Figure 12 at Y = 0 cm.

Figures 13 through 15 show the temperature profiles of the system when the plastic shield is added to the last case. Due to its minimal effect on the overall heat transfer process, no greater heat input is allowed. The TATB temperatures are slightly higher within the shield boundary.

## Conclusions

Heat transfer into a TATB charge is an extremely slow process. In the one-dimensional model, raising the TATB temperature from 20$^oC$ to 100$^oC$ at 1 cm depth while maintaining the surface temperature within 250$^oC$ requires more than 3 minutes.

The required heating time is reduced to 30 secs when a conical cavity filled with TATB is heated in three directions. However, the increased temperature in the center region alone may be insufficient in achieving total detonation of the TATB charge. Experiments relating the detonation characteristics to the preheating of TATB in selected regions are required before we can identify a workable configuration.

Thin aluminum discs embedded in the TATB charge further improve the heat conduction process. Desirable temperature distributions are reached in 10-15 secs. The effects of the metal discs on the detonation waves have to be examined. A thin layer of insulating material surrounding the region of interest raises the temperature in that region slightly. Its contribution to the overall heating process is limited, however. By accelerating the heat transfer process, the modified systems greatly reduces the heat dissipation and thus the total energy required. While the basic system consumes 955 cal in the first three minutes, the modified charge holder with two aluminum discs requires only 385 cals in the first 10 secs.

References

[1]R. K. Jackson, et.al., "Initiation and Detonation Characteristics of TATB", Sixth Symposium on Detonation, San Diego, CA, August 1976.

[2]P. J. Schneider, "Conduction Heat Transfer", Addison-Wesley, 1955.

Figure 4. Temperature history at selected locations - no shield, no conductor

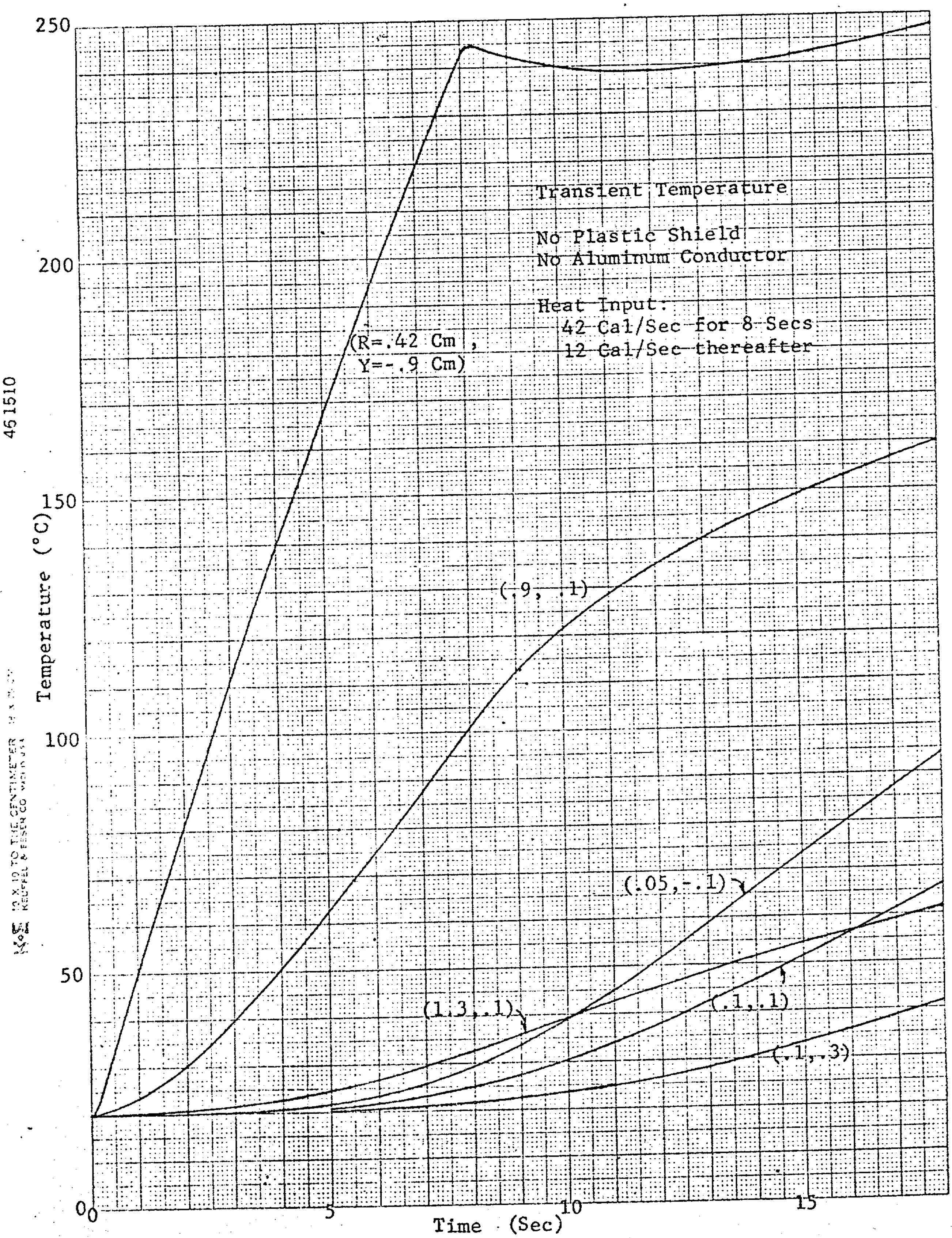

Figure 5. Radial temperature distribution at 15 secs - no shield, no conductor

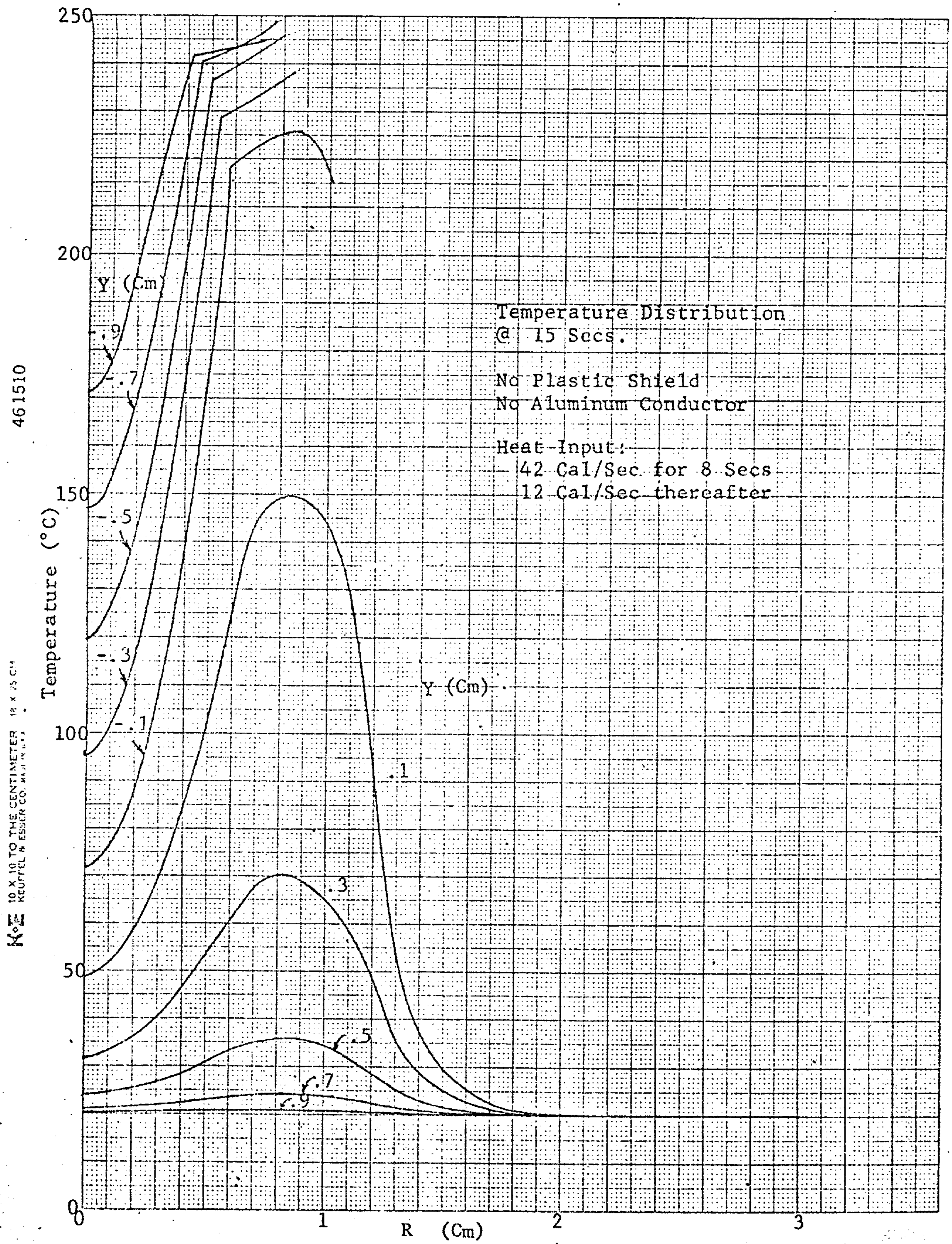

Figure 6. Axial temperature distribution at 15 secs - no shield, no conductor

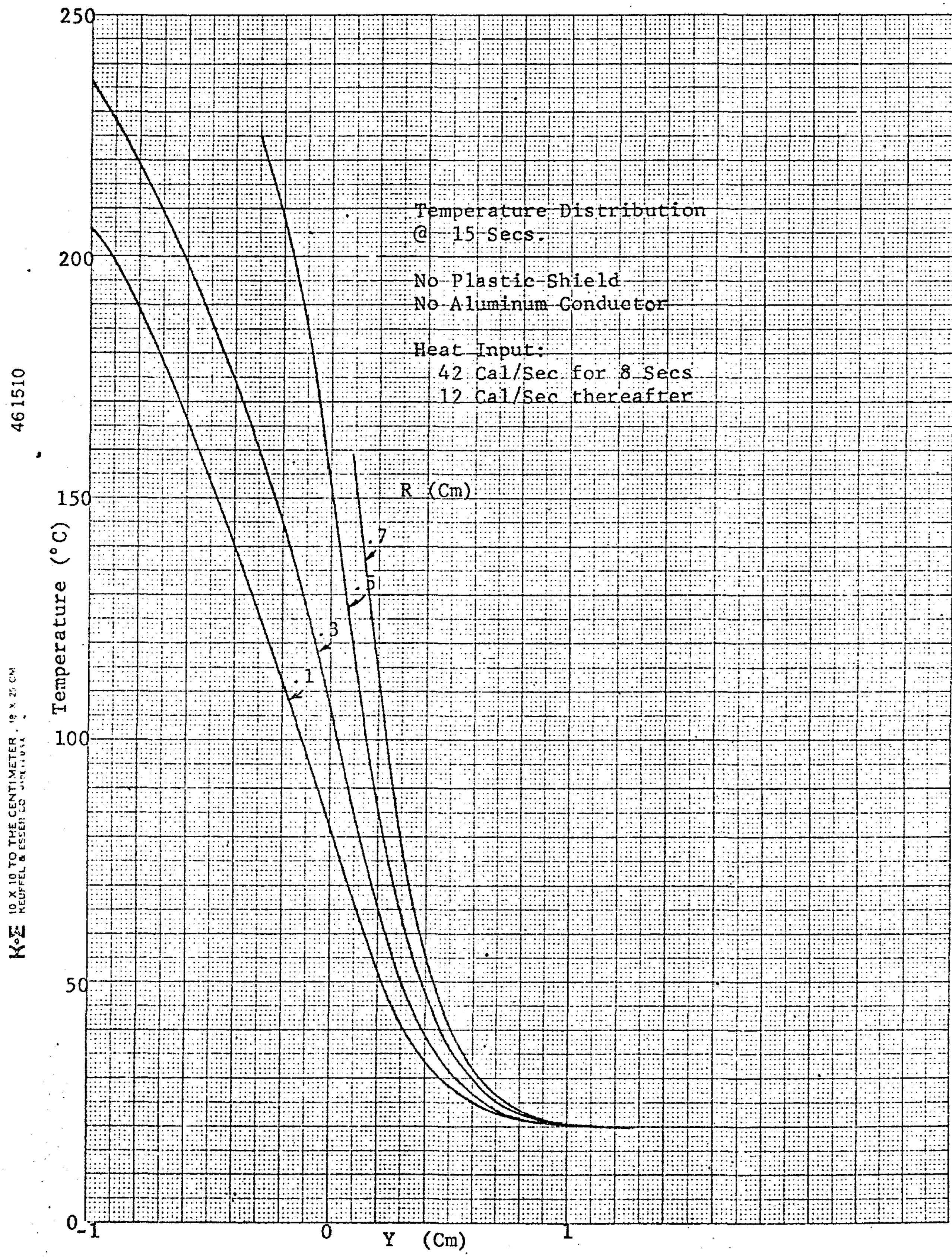

Figure 7. Temperature history at selected locations - no shield, no conductor

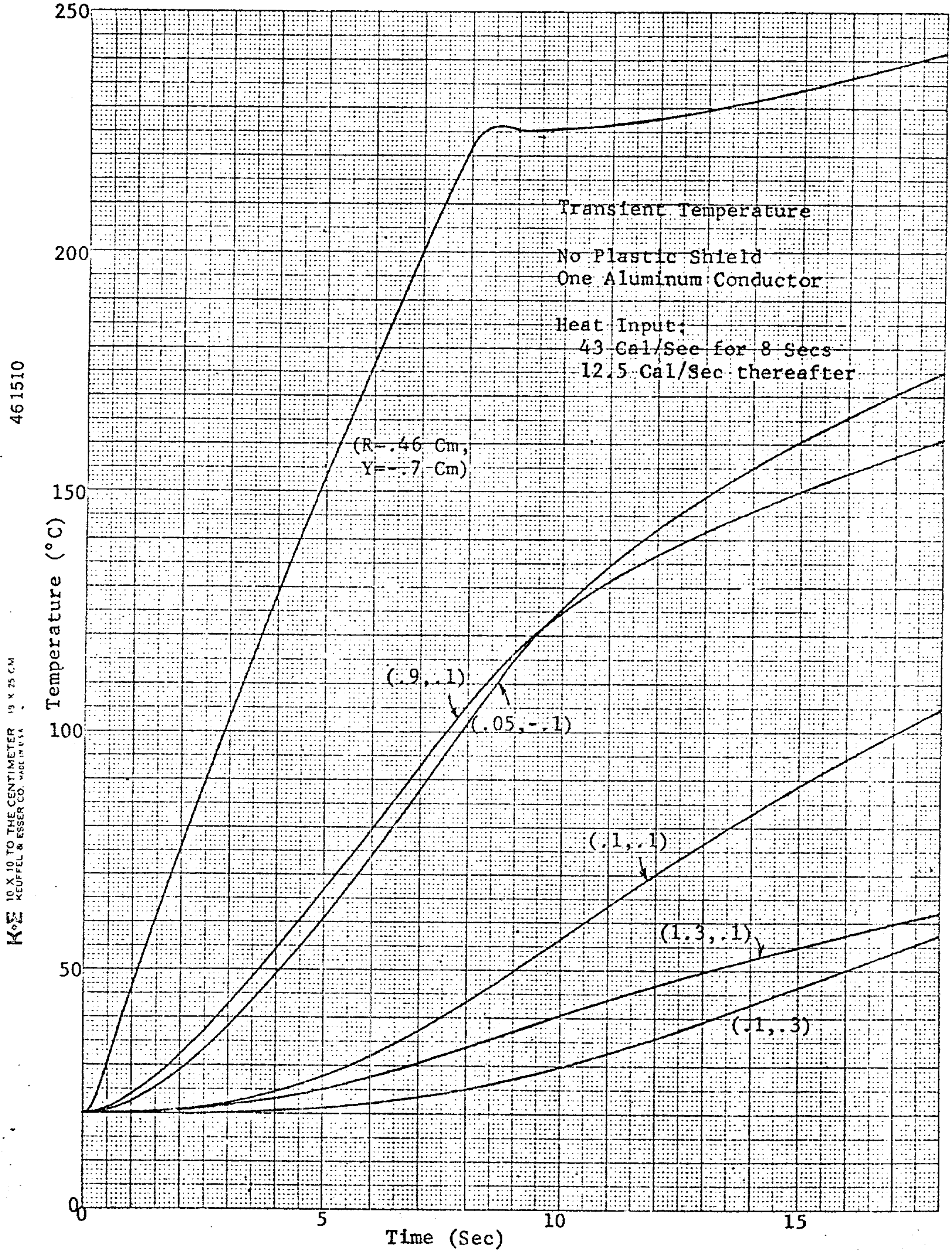

Figure 8. Radial temperature distribution at 15 secs - no shield, no conductor

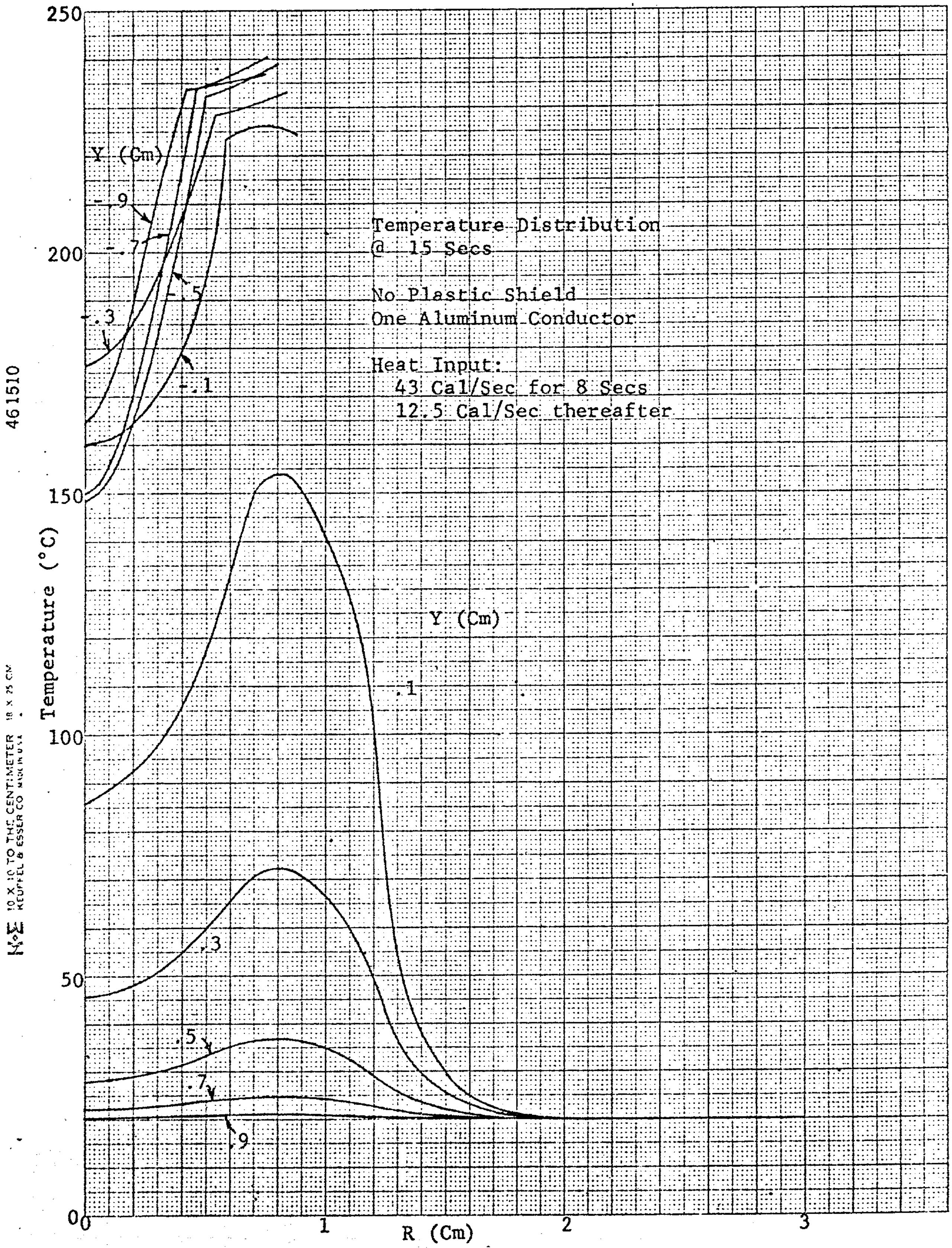

Figure 9. Axial temperature distribution at 15 secs no shield, no conductor

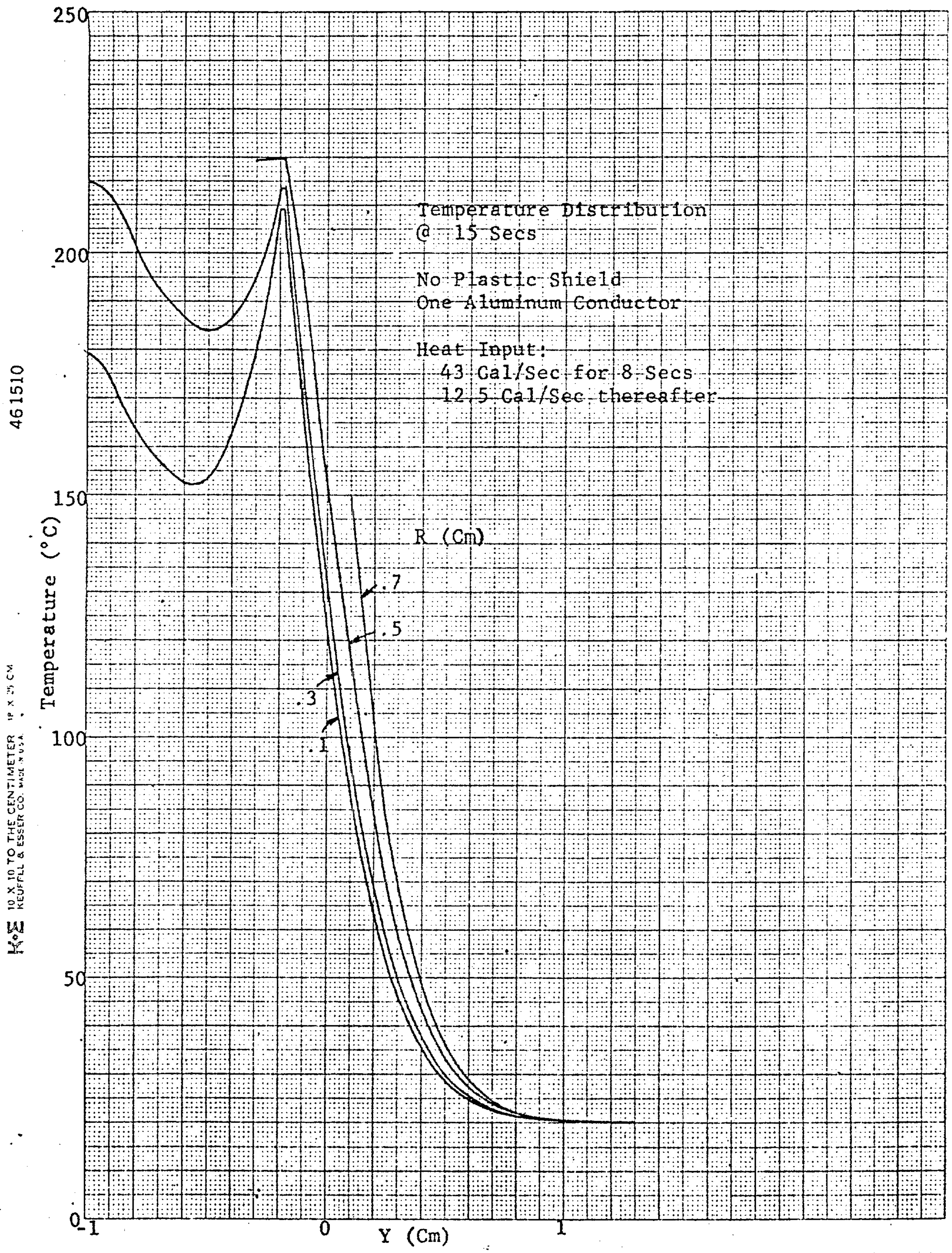

Figure 10. Temperature history at selected locations - no shield, two conductors

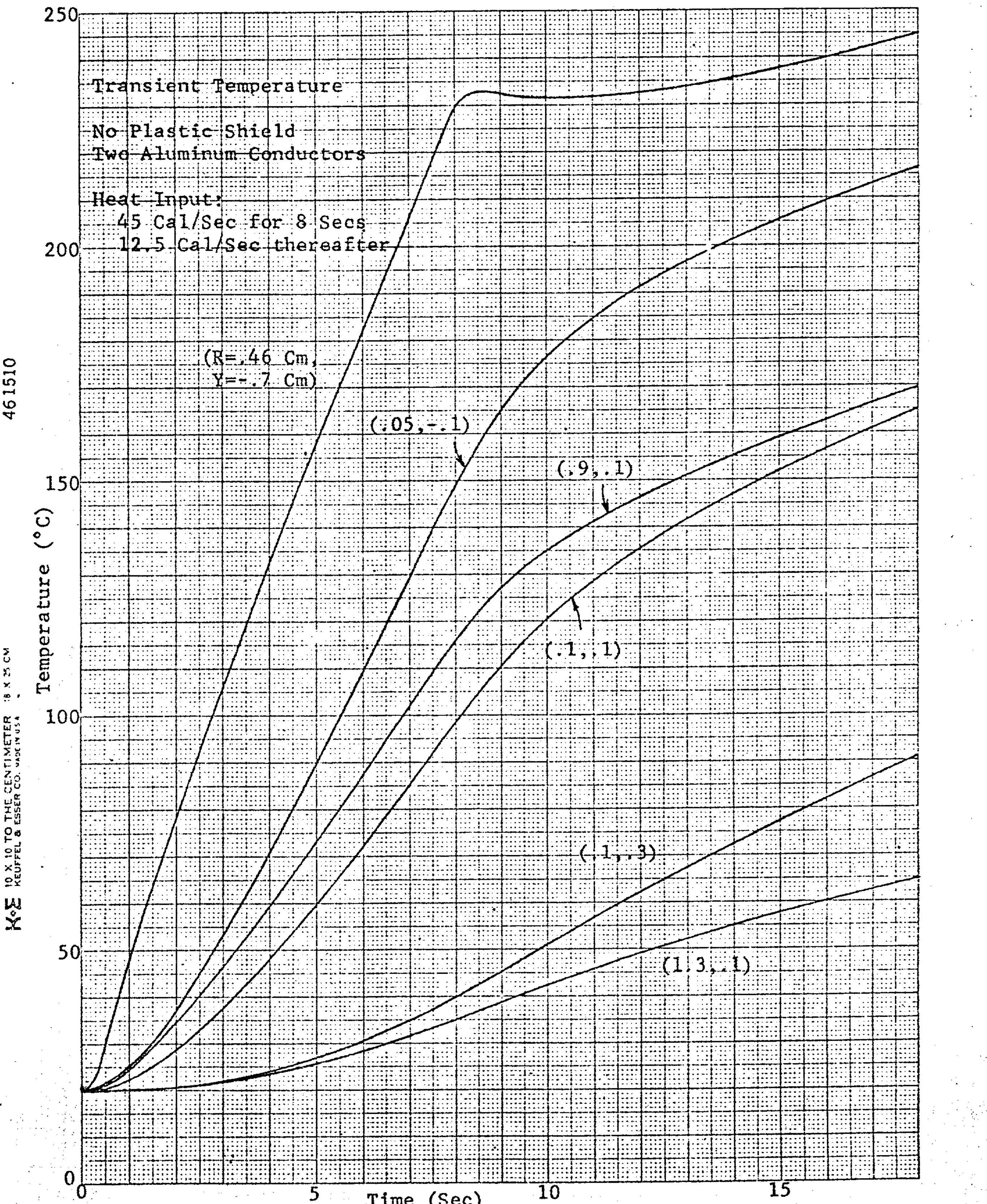

Figure 11. Radial temperature distribution at 15 secs - no shield, two conductors

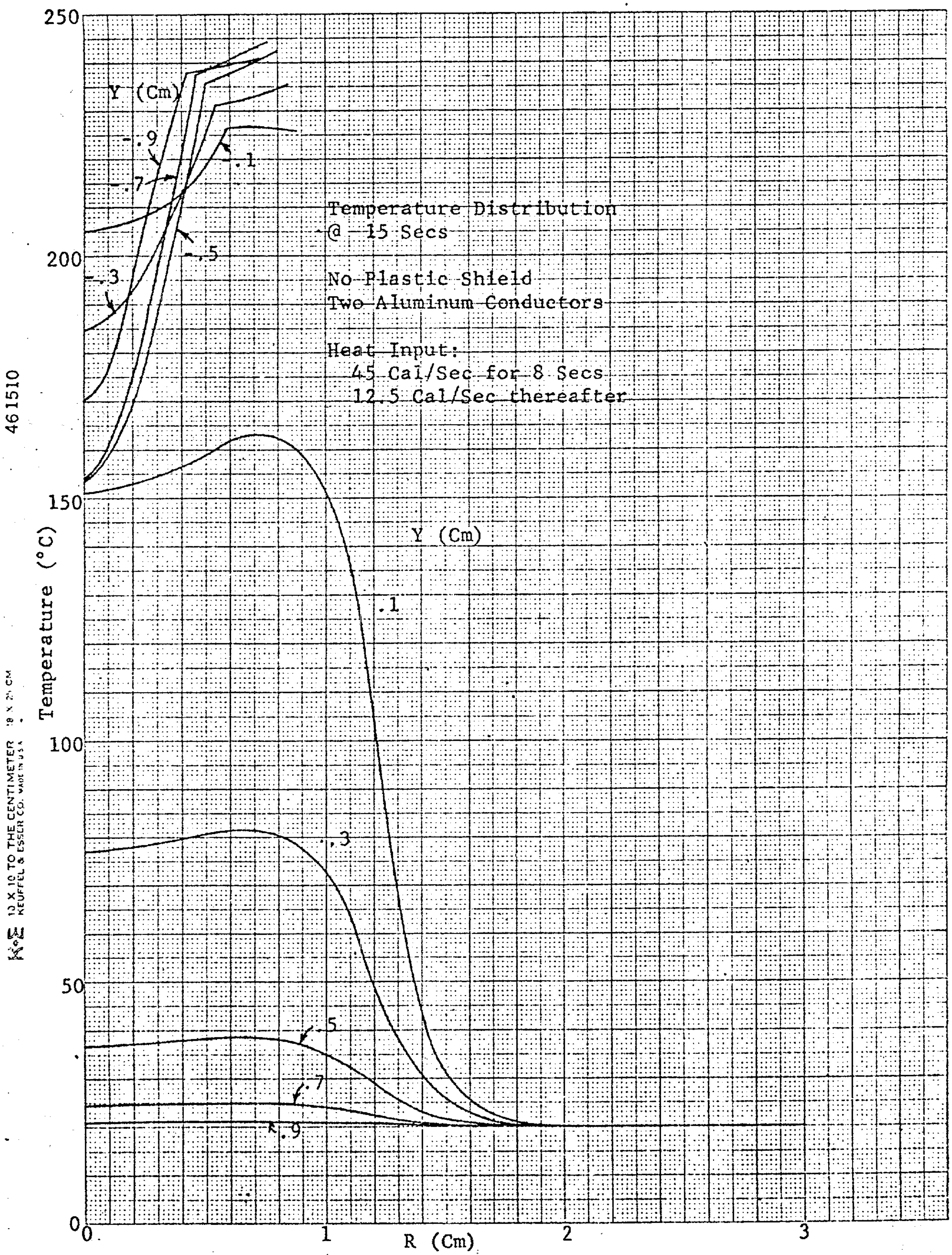

Figure 12. Axial temperature distribution at 15 secs - no shield, two conductors

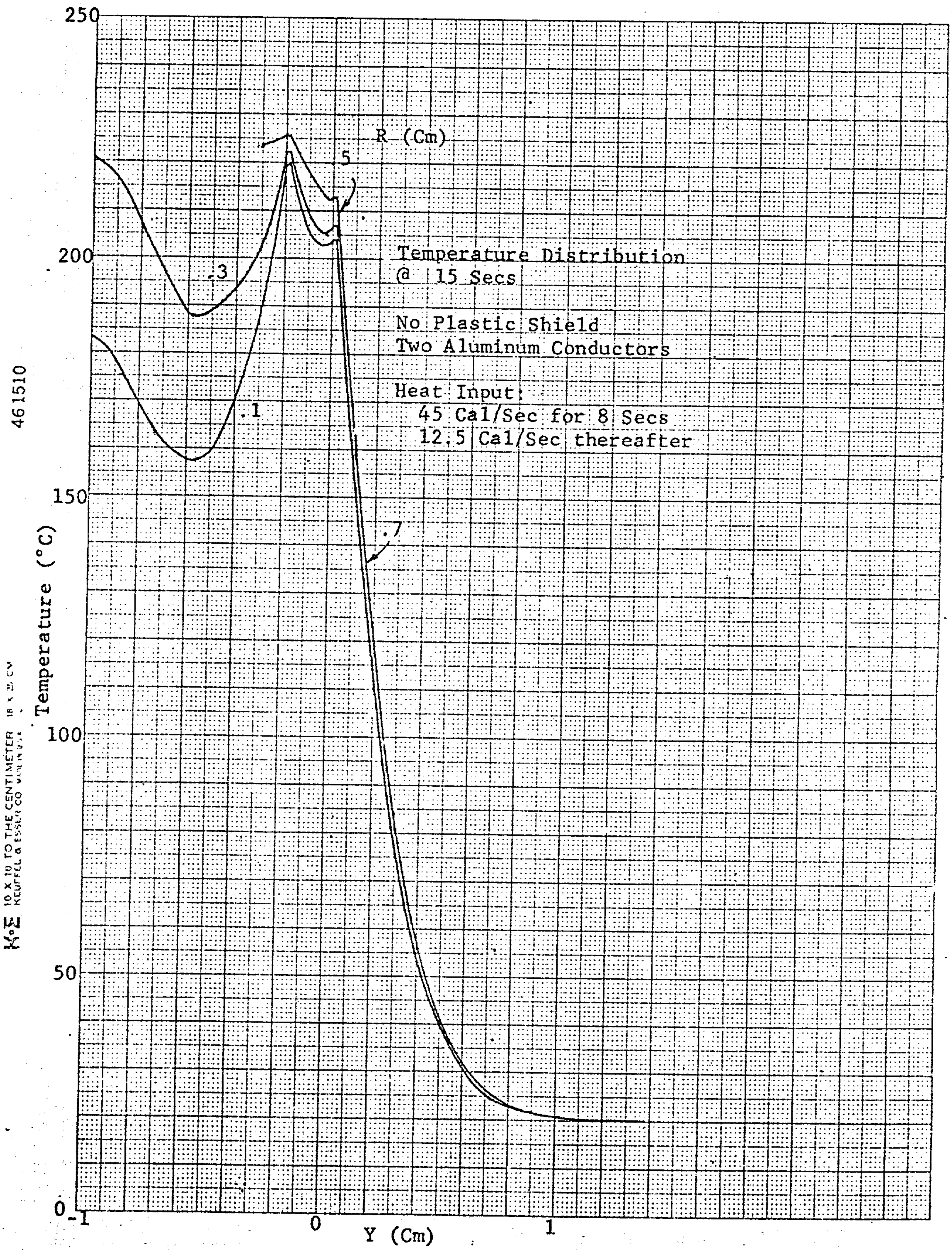

Figure 13. Temperature history at selected locations - shield, two conductors

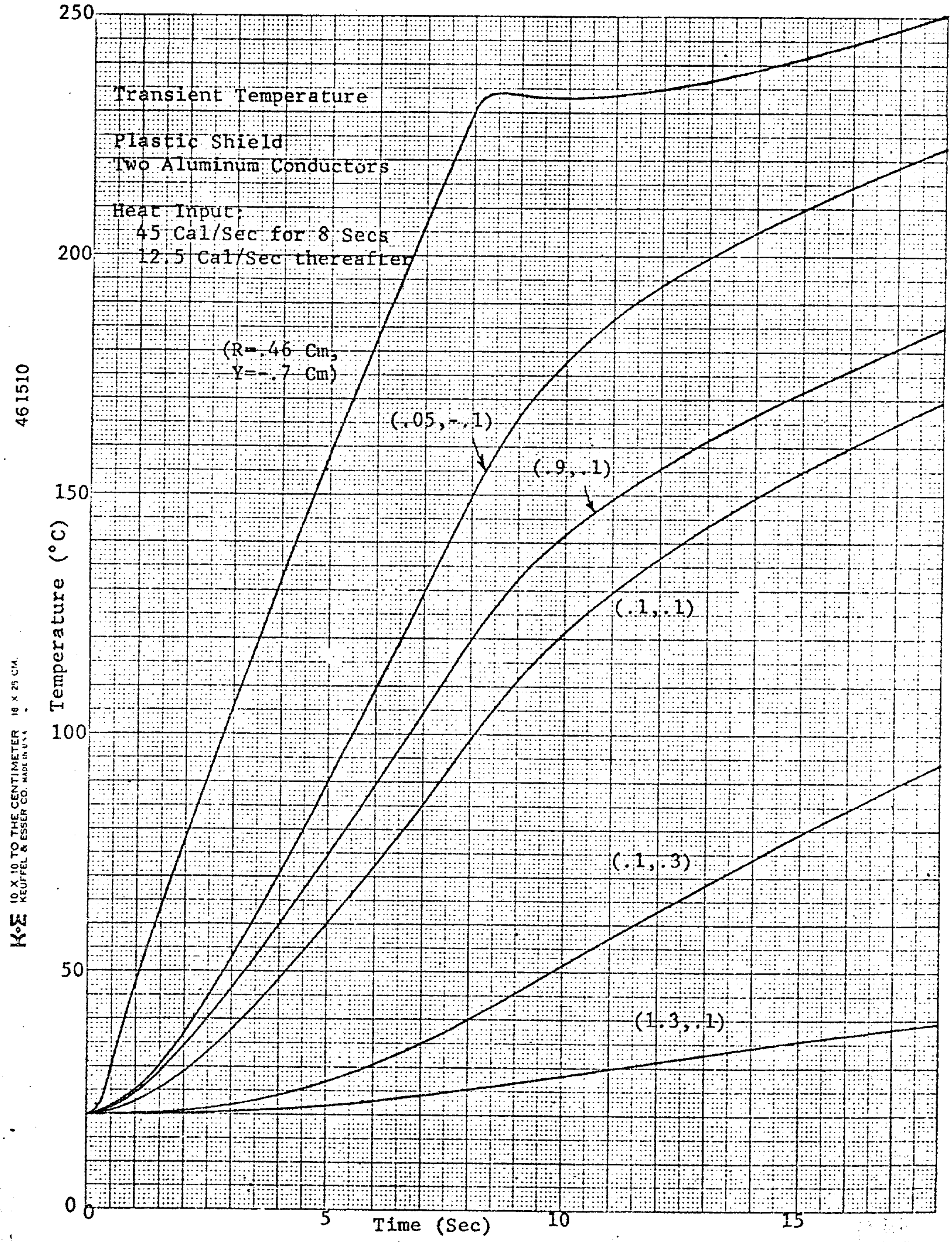

Figure 14. Radial temperature distribution at 15 secs - shield, two conductors

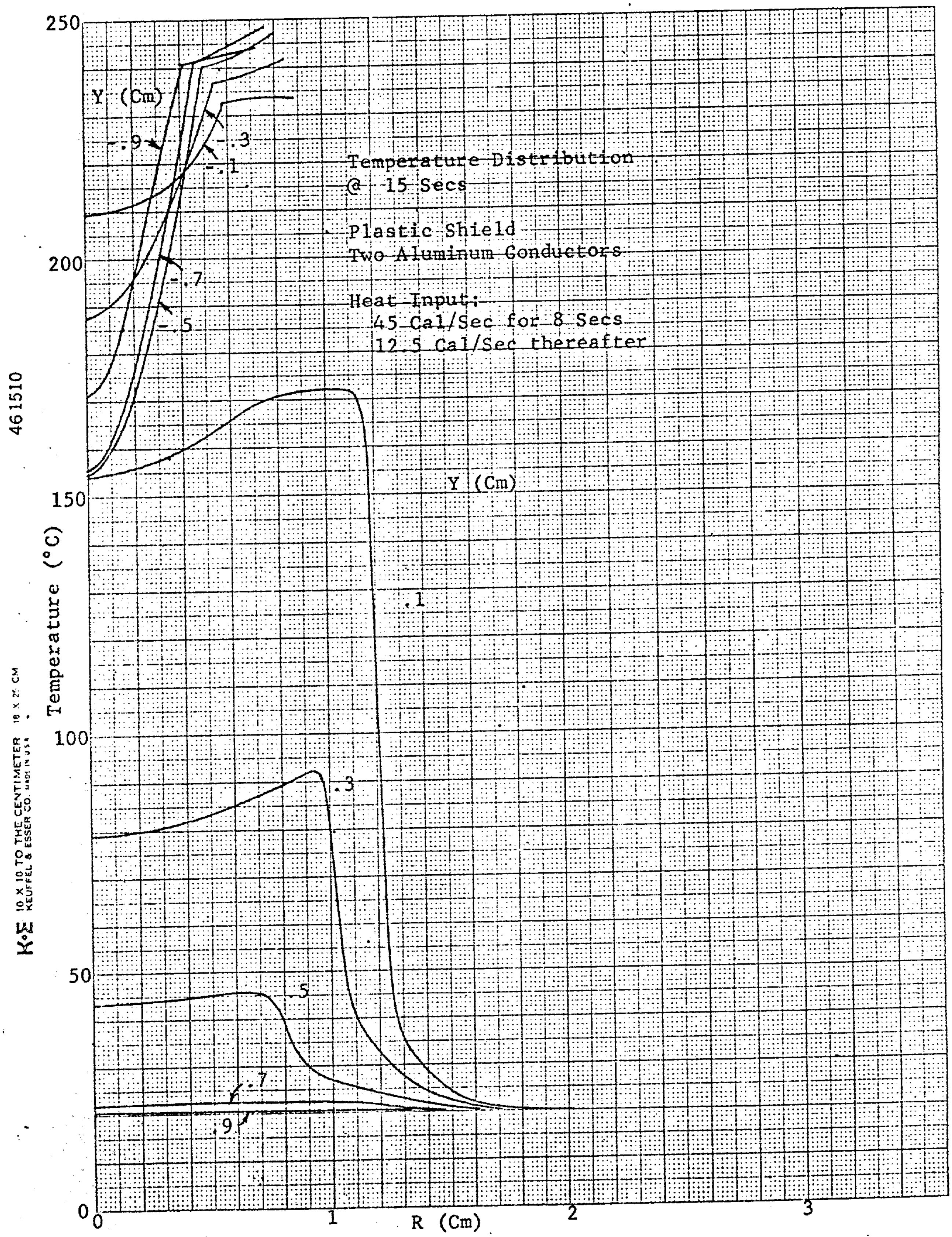

Figure 15. Axial temperature distribution at 15 secs - shield, two conductors

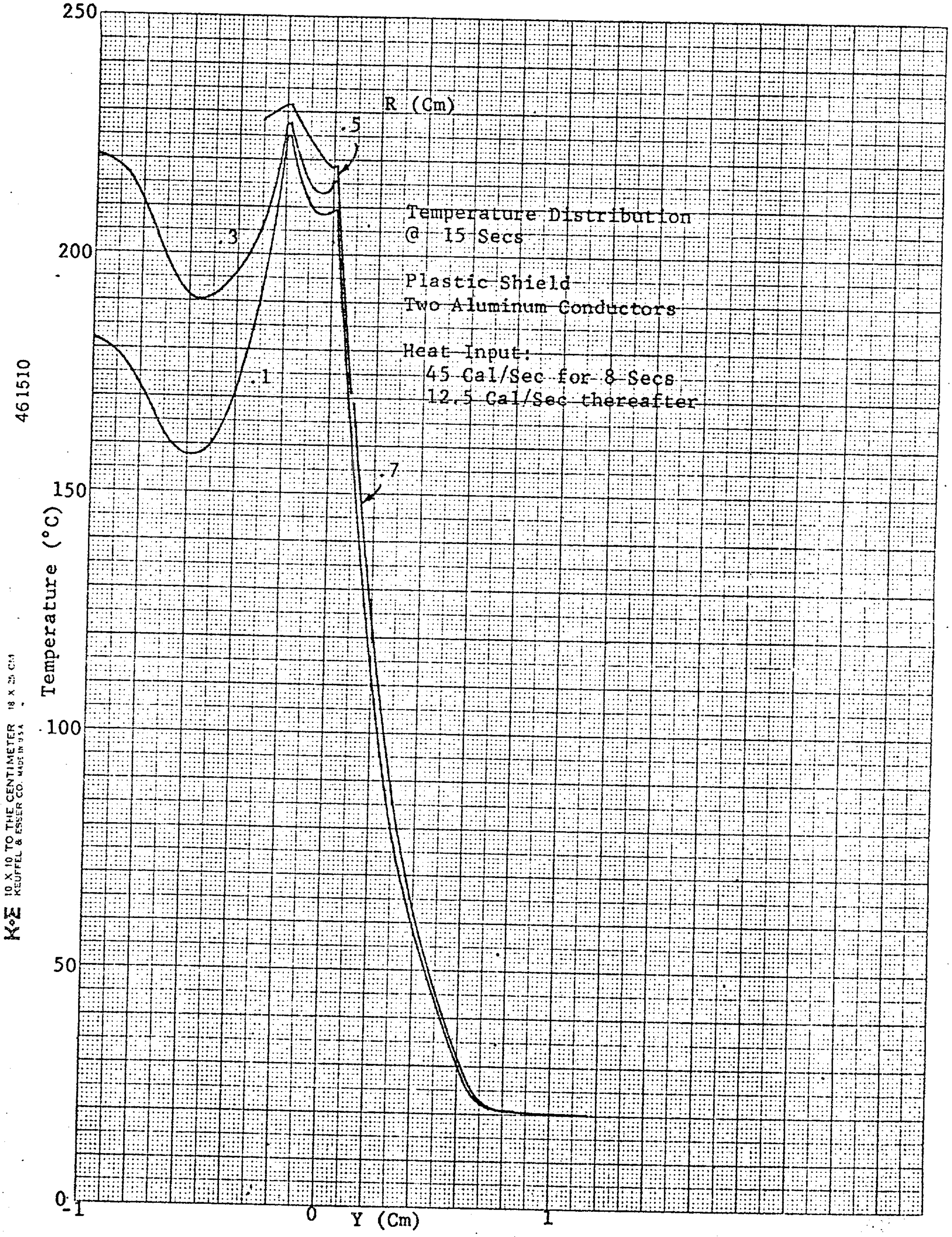

## DISTRIBUTION

LLL

J. R. Stroud
R. C. Weingart

Mound

J. R. Brinkman
R. D. DeSando
H. L. Turner
M. A. Witzerman
T. S. Chou
Document Control